Corresponding Author: Dr. Josep Vicent Mercader,

Corresponding Author's Institution: IATA-CSIC

First Author: Eric Ceballos-Alcantarilla

Order of Authors: Eric Ceballos-Alcantarilla; Consuelo Agulló; Antonio Abad-Somovilla; Antonio Abad-Fuentes; Josep Vicent Mercader

Research Data Related to this Submission

There are no linked research data sets for this submission. The following reason is given:
Data will be made available on request

1 # Highly sensitive monoclonal antibody-based

2 # immunoassays for the analysis of fluopyram in food

3 # samples

4   Eric Ceballos-Alcantarilla[a], Consuelo Agulló[a], Antonio Abad-Somovilla[a], Antonio Abad-Fuentes[b],

5   Josep V. Mercader[b,*]

6   [a] Department of Organic Chemistry, University of Valencia, Doctor Moliner 50, 46100

7   Burjassot, Valencia, Spain

8   [b] Institute of Agrochemistry and Food Technology (IATA), Spanish Research Council (CSIC),

9   Agustí Escardino 7, 46980 Paterna, Valencia, Spain

10   * Corresponding author: Tel. +34-963900022; Fax +34-963636301; E-mail

11   jvmercader@iata.csic.es

12

13

14

15

Abstract

Monoclonal antibody-based techniques have become a useful analytical technology in the agro-food sector. Nowadays, residues of the recently registered fungicide fluopyram are increasingly being found in quality control programs. In the present study, novel chemical derivatives of this pesticide were prepared and specific and high-affinity monoclonal antibodies to fluopyram were raised for the first time. Moreover, immunoassays to fluopyram were developed in two alternative enzyme-linked immunosorbent assay formats, using homologous and heterologous assay conjugates, with limits of detection below 0.05 μg L^{-1}. The optimized immunoassays were applied to the analysis of fluopyram in fortified plums and grapes of four different varieties as well as in in-house prepared musts and wines. Recoveries were between 76.3% and 109.6% and coefficients of variation were below 20%. Quantification limits were well below the maximum residue limits. Immunoassay performance was statistically validated with a reference chromatographic technique using samples from fluopyram-treated plum and grape cultivars.

Keywords

Fluopyram; Hapten; ELISA; Food safety; Stone fruits; Grapes; Must; Wine

Chemical compounds studied in this article

Fluopyram (PubChem CID: 11158353); Penthiopyrad (PubChem CID: 11388558); Fluxapyroxad (PubChem CID: 16095400); Fluopicolide (PubChem CID: 11159021).

1. Introduction

Succinate dehydrogenase inhibitors (SDHI) were first used in the late 1960s to fight fungal pests. The target enzyme, also called complex II, is a fundamental constituent of the mitochondrial respiration chain and the Krebs cycle (Avenot & Michailides, 2010). In recent years, new-generation SDHI fungicides with extended biocide properties have been developed. Due to their unique site of action, these compounds show no cross-resistance with other chemical classes such as strobilurin and anilinopyrimidine fungicides. Novel SDHI active principles comprise boscalid, penthiopyrad, fluxapyroxad, and fluopyram, which are characterized by lower toxicity to non-target organisms, higher efficiency, and broader spectrum of anti-fungal activity. Fluopyram, a pyridylethylamide, was first commercially registered in the United States in 2012 (Proffer, Lizotte, Rothwell, & Sundin, 2013) and approved for use in the European Union in 2013 (European Commission Regulation, 2013). Structurally, it is characterized by a diaryl aromatic system with two trifluoromethyl substituents and an ethylene bridge (Fig. 1a). This bioactive compound shows low toxicity to mammals; the oral LD_{50} in rats is >2 g kg^{-1} (Pfeil & Boobis, 2010), though neurotoxic and reproductive effects cannot be discarded in humans (Pesticide Properties Database, 2019). The proposed acceptable daily intake and the acute reference dose have been set at 0.01 mg kg^{-1} and 0.5 mg kg^{-1}, respectively (European Food Safety Authority, 2011 and 2013). Fluopyram is nowadays commercialized by Bayer Cropscience under the name of Luna® as single or combined formulates. Particularly, Luna® Experience, with 20% (w/v) fluopyram and 20% (w/v) tebuconazole as active ingredients, was developed to control intricate plant diseases caused by fungal pathogens. This fungicide is recommended to treat major crops such as grapes, stone

62 fruits, and vegetables for the control of grey mould (botrytis), white mould

63 (sclerotinia), powdery mildew, and other diseases that are responsible for food quality

64 losses. In 2013, residues of fluopyram appeared for the first time in the European

65 Pesticide Monitoring Program, particularly in apples, lettuce, peaches, strawberries,

66 tomatoes, and wine (European Food Safety Authority, 2015).

67 A few years ago, Polgár et al. reported the analysis of fluopyram and other

68 chemicals in food samples by high-performance liquid chromatography (HPLC) coupled

69 to high-resolution mass spectrometry (MS) (Polgár et al., 2012). Most of the studies

70 that were published afterwards for the analysis of fluopyram employed a liquid

71 chromatographic technique with MS and tandem MS detection (Yang et al., 2015;

72 Dzuman, Zachariasova, Veprikova, Godula, & Hajslova, 2015; Gan et al., 2016). Gas

73 chromatography-based methods with electron capture or MS detection have also been

74 developed (Lozano, Kiedrowska, Scholten, de Kroon, de Kok, & Fernández-Alba, 2016;

75 Lee et al., 2017). Moreover, multiresidue methods for the simultaneous analysis of

76 SDHI fungicides have recently been published (Abad-Fuentes, Ceballos-Alcantarilla,

77 Mercader, Agulló, Abad-Somovilla, & Esteve-Turrillas, 2015).

78 Nowadays, antibody-based techniques provide complementary strategies for

79 the analysis of chemical residues or contaminants in food. These methods are rapid

80 and sensitive, and can be developed in a variety of formats for economic, portable,

81 and/or easy-to-use applications. In order to generate high-affinity antibodies to a small

82 chemical, a functionalized mimic of the target compound (hapten) must be covalently

83 coupled to a larger immunogenic molecule. Monoclonal antibodies are generally

84 preferred for analytical purposes. Afterwards, antibodies can be incorporated into

85   adequate analytical platforms. The most accepted immunochemical method for the

86   analysis of small molecules is the competitive enzyme-linked immunosorbent assay

87   (cELISA), mostly developed in two alternative formats; the antibody-coated format

88   with direct detection and the conjugate-coated format with indirect detection.

89   Competition is frequently achieved with a covalent protein conjugate of an analogue

90   of the target compound. This hapten can be the same as that employed for

91   immunization (homologous hapten) or it can contain molecular differences

92   (heterologous hapten) which may enhance assay sensitivity.

93   In a previous study, polyclonal antibodies to fluopyram were reported

94   (Ceballos-Alcantarilla, Agulló, Abad-Fuentes, Abad-Somovilla, & Mercader, 2015). The

95   aim of the present study was to develop and validate highly sensitive monoclonal

96   antibody-based immunoassays for the analysis of fluopyram residues in food samples.

97   A collection of fluopyram haptens was synthesized and high-affinity monoclonal

98   antibodies specific of this compound were generated for the first time. Hapten

99   conjugates with a variety of heterologies were prepared in order to study their

100 influence on the performance of monoclonal antibody-based cELISA. The developed

101 immunoassays were applied to the analysis of fluopyram in fruit samples, particularly

102 plums and grapes, as well as processed food products such as musts and wines.

103 Fortified food samples and contaminated samples from fruit and vine cultivars were

104 employed for the characterization and validation of the developed immunochemical

105 assays by comparison with a reference chromatographic technique.

106 **2. Materials and methods**

107 *2.2. Reagents and instruments*

108   General experimental procedures and techniques for the synthesis and

109   characterization of haptens are reported in the Supplementary Data file. Compounds

110   used in this study present minor safety concerns; however, it is advisable to work in a

111   well-ventilated fume hood during synthesis work. Pestanal® grade fluopyram (*N*-(2-(3-

112   chloro-5-(trifluoromethyl)-2-pyridyl)ethyl)-α,α,α-trifluoro-*o*-toluamide, CAS number

113   658066-35-4, Mw 396.7) and other pesticide analytical standards were purchased from

114   Fluka/Riedel-de-Haën (Seelze, Germany). Stock solutions were prepared in anhydrous

115   *N*,*N*-dimethylformamide and kept at −20 °C in amber glass vials. Luna® Experience

116   suspension was kindly provided by Bayer Cropscience (Frankfurt, Germany). Bovine

117   serum albumin (BSA) fraction V was obtained from Roche Applied Science (Mannheim,

118   Germany). Horseradish peroxidase (HRP), ovalbumin (OVA), foetal bovine serum,

119   hybridoma fusion and cloning supplement, and Freund's adjuvants were from

120   Sigma/Aldrich (Madrid, Spain). Hapten density of protein conjugates was determined

121   with a 5800 matrix-assisted laser desorption ionization time-of-flight (MALDI-TOF/TOF)

122   mass spectrometry apparatus from AB Sciex (Framingham, MA, USA). HiTrap™ protein

123   G HP columns for mouse IgG purification were procured from GE Healthcare (Uppsala,

124   Sweden).

125   Immunoassays were carried out with Costar® 96-well flat-bottom high-binding

126   polystyrene ELISA plates from Corning (Corning, NY, USA). Peroxidase labelled rabbit

127   anti-mouse immunoglobulin polyclonal antibody (secondary antibody) was from Dako

128   (Glostrup, Denmark). *o*-Phenylenediamine and triphenylphosphate (TPP) were

129   obtained from Sigma/Aldrich (Madrid, Spain). Primary/secondary amine from Varian

130   (Palo Alto, CA, USA) and organic solvents from Scharlab (Barcelona, Spain) were used

131   for sample preparation. Microplate wells were washed with an ELx405 washer from

132 BioTek Instruments (Winooski, VT, USA). Immunoassay absorbance values were read

133 with a PowerWave HT microplate reader also from BioTek.

134   Fluopyram residues were determined by HPLC using a UPLC Acquity system

135 from Waters (Milford, MA, USA) furnished with a binary solvent delivery system, an

136 autosampler, and a BEH C18 (1.7 µm, 2.1 × 50 mm) column. An Acquity triple

137 quadrupole MS detector, also from Waters, with a Z-spray electrospray ionization

138 source (3.5 kV capillary voltage, and 120 °C and 300 °C source and desolvation

139 temperature, respectively) were employed for tandem mass acquisitions.

140   Fermentations were carried out in an incubator from Selecta (Barcelona, Spain)

141 using *Saccaromyces cerevisiae* cells from Lallemand Inc (Montreal, Quebec, Canada).

142 For density measurements, a Densito 30 PX densitometer from Mettler-Toledo GmbH

143 (Greifensee, Switzerland) was employed. Musts and wine composition was analysed

144 with a Surveyor Plus HPLC chromatography system from Thermo Fisher Scientific

145 (Waltham, MA, USA) equipped with refraction index and UV-vis detectors. A Hyper REZ

146 XP carbohydrate H+8 column, also from Thermo Fisher Scientific, was employed as

147 stationary phase at 50 °C. Samples were filtered with 0.2 µm nylon filter devices.

148   A series of buffers and solutions were employed. Coating buffer: 50 mM

149 carbonate–bicarbonate buffer, pH 9.6; PBS: 10 mM phosphate buffer, pH 7.4, with 140

150 mM NaCl; PBST: PBS containing 0.05% (v/v) Tween 20; PB: 100 mM sodium phosphate

151 buffer, pH 7.4; washing solution: 150 mM NaCl containing 0.05% (v/v) Tween 20;

152 enzyme substrate buffer: 25 mM citrate and 62 mM sodium phosphate buffer, pH 5.4.

153 *2.2. Hapten synthesis*

154   The structure of immunizing hapten FP*a* is shown in Fig. 1a and its preparation was

155 described in a previous article (Ceballos-Alcantarilla et al., 2015). The developed

156 synthetic sequence for the preparation of immunizing hapten FP*b* is depicted in Fig. 2.

157 Preparation of amino pyridine **8** is described in the Supplementary Data file (Fig. S1).

158 Details of all synthetic steps and characterization data of other intermediate

159 compounds can be found in the Supplementary Data file. Hapten FP*b* was obtained as

160 a white solid. Mp 107.8–109.3 °C (benzene); IR (neat) v_{max} (cm^{-1}) 3267s, 3071w,

161 3040w, 2948m, 2866m, 1717s, 1653s, 1545m, 1399w, 1331s, 1131s, 914m; ^{1}H NMR

162 (300 MHz, CDCl$_3$) δ 9.94 (br s, 1H, CO$_2$*H*), 8.65 (d, *J* = 1.2 Hz, 1H, *H$_6$* Py), 7.92 (d, *J* = 1.2

163 Hz, 1H, *H$_4$* Py), 7.43 (d, *J* = 1.1 Hz, 1H, *H$_2$* Ph), 7.42 (d, *J* = 8.0 Hz, 1H, *H$_5$* Ph), 7.35 (dd, *J* =

164 8.0, 1.1 Hz, 1H, *H$_6$* Ph), 6.69 (t, *J* = 5.9 Hz, 1H, CON*H*), 3.99 (dt, *J* = 5.9, 5.9 Hz, 2H,

165 NHC*H$_2$*CH$_2$), 3.30 (t, *J* = 5.9 Hz, 2H, NHCH$_2$C*H$_2$*), 2.66 (t, *J* = 7.6 Hz, 2H, *H$_6$*), 2.34 (t, *J* = 7.4

166 Hz, 2H, *H$_2$*), 1.66 (tt, *J* = 7.4, 6.0 Hz, 2H, *H$_3$*), 1.63 (tt, *J* = 7.6, 6.0 Hz, 2H, *H$_5$*), 1.45–1.29

167 (m, 2H, *H$_4$*); ^{13}C NMR (75 MHz, CDCl$_3$) δ 179.3 (s, *C$_1$*), 168.2 (s, *C*ONH), 160.8 (s, *C$_2$* Py),

168 144.9 (s, *C$_1$* Ph), 143.6 (q, $^3J_{CF}$ = 4.0 Hz, *C$_6$* Py), 134.1 (q, $^3J_{CF}$ = 3.6 Hz, *C$_4$* Py), 133.4 (q,

169 $^3J_{CF}$ = 2.1 Hz, *C$_4$* Ph), 132.1 (s, *C$_3$* Py), 132.0 (s, *C$_6$* Ph), 128.9 (s, *C$_5$* Ph), 127.1 (q, $^2J_{CF}$ =

170 31.6 Hz, *C$_3$* Ph), 126.3 (q, $^3J_{CF}$ = 4.8 Hz, *C$_2$* Ph), 126.1 (q, $^2J_{CF}$ = 33.8 Hz, *C$_5$* Py), 123.7 (q,

171 $^1J_{CF}$ = 274.1 Hz, *C*F$_3$ Ph), 122.8 (q, $^1J_{CF}$ = 272.7 Hz, *C*F$_3$ Py), 37.0 (s, NH*C*H$_2$CH$_2$), 35.4 (s,

172 *C$_6$*), 34.2 (s, NHCH$_2$*C*H$_2$), 33.9 (s, *C$_2$*), 30.8 (s, *C$_5$*), 28.5 (s, *C$_4$*), 24.5 (s, *C$_3$*); ^{19}F NMR (282

173 MHz, CDCl$_3$) δ −59.35 (s, C*F$_3$* Ph), −62.73 (s, C*F$_3$* Py); HRMS (TOF, ES+) *m/z* calcd for

174 $C_{22}H_{22}{}^{35}ClF_6N_2O_3$ [M+H]$^+$ 511.1218, found 511.1196; UV (PB) ε (290 nm) = 0.13 mM^{-1}

175 cm^{-1}, ε (280 nm) = 2.45 mM^{-1} cm^{-1}, ε (270 nm) = 4.70 mM^{-1} cm^{-1}, ε (260 nm) = 3.35

176 mM^{-1} cm^{-1}, ε (250 nm) = 2.56 mM^{-1} cm^{-1}.

177   The synthetic strategies used for the preparation of haptens FP*ha* and FP*hb*

178   (Fig. 1a) are depicted in Fig. S2 and S3. Experimental details and characterization data

179   of all compounds are reported in the Supplementary Data file.

180   *2.3. Bioconjugate preparation*

181   Previously to coupling, active esters of the haptens were prepared by reaction

182   of the free carboxylic group with *N,N*-disuccinimidyl carbonate and Et$_3$N in CH$_3$CN at

183   room temperature (Fig. 2, S2, and S3), following a procedure applied in our laboratory

184   in previous studies (Esteve-Turrillas, Parra, Abad-Fuentes, Agulló, Abad-Somovilla, &

185   Mercader, 2010). *N*-Hydroxysuccinimidyl esters were readily purified by flash column

186   chromatography. Purified active esters were fully characterized by spectroscopic

187   methods (for details see the Supplementary Data file).

188   All of the synthetic haptens were covalently coupled to OVA and HRP, and

189   hapten FP*b* was also linked to BSA, using the corresponding purified active esters.

190   Conjugates of hapten FP*a* had been equivalently prepared in a previous study

191   (Ceballos-Alcantarilla et al., 2015). Briefly, purified succinimide esters of the haptens

192   were dissolved in anhydrous *N,N*-dimethylformamide and dropwise added to protein

193   solutions in 50 mM carbonate buffer, pH 9.6, at a ratio of 24, 8, and 10 mol per mol of

194   BSA, OVA, and HRP, respectively, and the mixtures were gently stirred 2 h at room

195   temperature. Bioconjugates were purified by gel filtration chromatography with a 15

196   mL Sephadex G-25 column using PB as eluent at 5 mL min^{-1}. BSA conjugates were filter

197   sterilized, brought to 1 mg mL^{-1} with sterile PB, and stored frozen at −20 °C, OVA

198   conjugates were diluted with PB and stored at −20 °C with 0.01% (w/v) thimerosal, and

199   HRP conjugates were 1:1 diluted with PBS containing 1% (w/v) BSA and 0.02% (w/v)

200   thimerosal, and stored at 4 °C. The obtained hapten-to-protein molar ratio (MR) was

201   determined by MALDI-TOF mass spectrometry after extensive dialysis of the

202   bioconjugate in MilliQ water (see the Supplementary Data file).

203   *2.4. Monoclonal antibody generation*

204   Experimental design was approved by the Bioethics Committee of the

205   University of Valencia. Animal manipulation was performed in compliance with the

206   European Directive 2010/63/EU and the Spanish laws and guidelines (RD1201/2005

207   and 32/2007) concerning the protection of animals used for scientific purposes. Two

208   sets of four mice were immunized with BSA–FP*a* or BSA–FP*b* conjugate by

209   intraperitoneal injections using Freund adjuvants. Details of the immunization

210   procedures can be found in the Supplementary Data file. For each immunogen, two

211   cell fusions were carried out; each of them employing the spleen cells from two

212   equally immunized mice. Hybridomas were generated using PEG1500 as fusing agent

213   and they were grown following regular protocols (Mercader, Suárez-Pantaleón, Agulló,

214   Abad-Somovilla, & Abad-Fuentes, 2008a). Hybridoma culture supernatants were

215   screened, twelve days after cell fusion, following a double screening procedure

216   consisting of a differential cELISA using 100 nM fluopyram, followed by a checkerboard

217   cELISA, both of them with the homologous OVA coating conjugate (the conjugate

218   carrying the same hapten as the immunizing conjugate) (Mercader, Suárez-Pantaleón,

219   Agulló, Abad-Somovilla, & Abad-Fuentes, 2008b). Further information is provided in

220   the Supplementary Data file. High-affinity antibody producing hybridomas were cloned

221   by limiting dilution in hypoxanthine–thymidine medium containing 20% (v/v) foetal

222   bovine serum and 1% (v/v) hybridoma fusion and cloning supplement. Stable clones

223 were expanded and cryopreserved in liquid nitrogen. Immunoglobulins were purified

224 from late stationary-phase culture supernatants by ammonium sulphate precipitation

225 and affinity chromatography with protein G. Purified monoclonal antibodies were

226 stored as ammonium sulphate precipitates at 4 °C.

227 *2.5. Antibody-coated direct competitive ELISA*

228 Microplates were coated with 100 µL per well of antibody solution in coating

229 buffer by overnight incubation at 4 °C. Then, microwells were washed four times with

230 washing solution. The competitive reaction was carried out during 1 h at room

231 temperature by sequentially adding 50 µL per well of fluopyram standard solution in

232 PBS plus 50 µL per well of HRP tracer solution in PBST. After washing the wells as

233 before, the enzymatic activity was revealed at room temperature with 100 µL per well

234 of a freshly prepared 2 mg mL^{-1} *o*-phenylenediamine solution in enzyme substrate

235 buffer containing 0.012% (v/v) H_2O_2. The reaction was stopped after 10 min with 100

236 µL per well of 1 M H_2SO_4 and the absorbance was immediately read, in a dual

237 wavelength mode, at 492 nm using 650 nm as the reference wavelength.

238 *2.6. Conjugate-coated indirect competitive ELISA*

239 Coating was performed with 100 µL per well of OVA conjugate solution in

240 coating buffer by overnight incubation at room temperature. After washing the plate

241 as described in section 2.5, the competitive reaction was carried out by mixing 50 µL

242 per well of fluopyram standard solution in PBS plus 50 µL per well of antibody solution

243 in PBST and incubation at room temperature during 1 h. Then, plates were washed as

244 before and 100 µL per well of a 1/2000 secondary antibody dilution in PBST was

245 added. After 1 h at room temperature, plates were washed again and the enzyme

246   activity was revealed and the absorbance was read as described for the direct assay

247   format.

248   *2.7. Sample preparation*

249   Plum trees and grapevines of different varieties (Garnacha, Bobal, Tempranillo,

250   and Macabeo) from the Utiel-Requena region (Spain) were treated at harvest season

251   with a Luna® Experience suspension prepared following the manufacturer instructions

252   and using a manual nebulizer. Two suspensions were prepared, one at the

253   recommended dose (treatment T1) of the active ingredient (0.038%, v/v) and the other

254   at a double concentration (treatment T2). Fruit blank samples were harvested before

255   the treatment. Fluopyram-containing samples were collected at different days after

256   fungicide application (D1 to D7 for plums and D1 and D3 for grapes). Then, stones from

257   plum samples were discarded, grape berries were separated from the stems, and the

258   fruits were chopped with a grinder. A fraction of grapes was destined to must and

259   wine preparation and the remaining fruit samples were used for pesticide extraction.

260   Blended grape berries were filtered to obtain must samples which were stored

261   at −20 °C until analysis. Wine samples were in-house prepared from musts to which a

262   portion of the solid fraction obtained after filtration was added as required for red

263   wine production, except for the Macabeo white must in order to produce white wine.

264   Then, 60 mL of must was inoculated with 2×10^{6} cells of *Saccaromyces cerevisiae* per

265   millilitre and incubated at 28 °C with continuous orbital agitation at 150 rpm. When

266   fermentation was finished, solids were discarded by centrifugation and wine samples

267   were stored at −20 °C until analysis.

268   Pesticides were extracted from plums and grapes by the standard QuEChERS

269   (Quick, Easy, Cheap, Effective, Rugged, and Safe) procedure as follows. Chopped

270   samples were further homogenized with an Ultra-Turrax blender from IKA (Staufen,

271   Germany) and 5 g of homogenate was mixed, in a 50-mL polypropylene centrifuge

272   tube, with 0.5 g of sodium acetate and 5 mL of acetonitrile containing 1% (v/v) acetic

273   acid and 500 µg L^{-1} of TPP as internal standard. Then, 2 g of anhydrous $MgSO_4$ was

274   added and vigorously stirred with a vortex during 1 min. After centrifugation at 2040×g

275   for 5 min, 1 mL of organic extract was collected in an Eppendorf tube and treated with

276   50 mg of primary/secondary amine and 150 mg of anhydrous $MgSO_4$. The formed

277   suspension was strongly vortex stirred during 1 min and centrifuged again at 6700×g

278   for 5 min. The supernatant was filtered through a Teflon membrane (0.2 µm of

279   diameter) and stored at −20 °C until analysis.

280   *2.8. Sample analysis*

281   For cELISA analysis, cleaned-up acetonitrile plum extracts and grape extracts of

282   the four varieties, as well as the corresponding must and wine samples were

283   conveniently diluted with MilliQ water and analysed by the optimized immunoassays.

284   Thus, five different fruit samples, four musts and four wines were evaluated. Eight-

285   point standard curves, including a blank, were prepared from a 50 µg L^{-1} fluopyram

286   solution in MilliQ water by six-fold serial dilution in water. Antibody or enzyme tracer

287   solutions were prepared in 2×PBS containing 0.05% (v/v) Tween 20. Experimental

288   values were fitted to a four-parameter logistic equation using the SigmaPlot software

289   package from SPSS Inc. (Chicago, IL, USA). Assay sensitivity was defined as the

290   concentration of analyte at the inflection point of the fitted curve, typically

291 corresponding to a 50% reduction (IC_{50}) of the maximum absorbance (A_{max}). The limit

292 of detection (LOD) was calculated as the concentration of analyte at a 10% drop of

293 A_{max}, and the linear range was estimated as the concentration range between a 20%

294 and 80% decrease of A_{max}. The limit of quantification (LOQ) for fluopyram residue

295 immunoanalysis in the studied food samples was defined as the lowest assayed

296 concentration for which recovery values between 80% and 120%, and coefficients of

297 variation (CV) below 20%, were obtained.

298 UPLC–MS/MS determinations were carried out with a multicomponent

299 calibration curve of 7 standards (0, 3, 10, 30, 100, 300, and 1000 µg L^{-1}) prepared by

300 serial dilution of fluopyram in acetonitrile containing 500 µg L^{-1} of TPP as internal

301 standard. A five microlitre sample was used and a binary mobile phase was applied at

302 400 µL min^{-1}, consisting of 0.5% (v/v) formic acid in MilliQ water (eluent A) and

303 acetonitrile (eluent B). Starting from a 50% (v/v) mixture of both eluents, elution was

304 carried out by linearly increasing eluent B, during 4 min, until a 95% (v/v) proportion

305 was reached, and then the mobile phase was maintained isocratic during 2 min. The

306 obtained retention times under the aforementioned conditions were 1.1 and 2.1 min

307 for fluopyram and TPP, respectively. Signal response was determined from the

308 quotient between the analyte peak area and that of the internal standard multiplied by

309 the concentration of the latter. Monitored ions were *m/z* 397 and 328, for fluopyram

310 and TPP, respectively. Weighted (1/x) least squares calibration curves were established

311 by linear regression of the signal and the concentration values of fluopyram. The LOD

312 value of the chromatographic method was calculated as $3s_0/b$, where s_0 is the standard

313 deviation (n = 10) of the signal at 3 µg L^{-1} of fluopyram and b is the slope of the

314 calibration curve.

315   **3. Results and discussion**

316   *3.1. Hapten design and synthesis*

317   A fundamental aspect for the generation of sensitive and specific antibodies

318   towards a small analyte is the way the hapten structure of the bioconjugate is

319   displayed to the immune system, which depends particularly on the linker tethering

320   site. In this study, which is directed to the production of monoclonal antibodies

321   suitable for the development of a sensitive immunoassay for the analysis of the

322   fungicide fluopyram, two haptens have been used for the preparation of the

323   immunogenic conjugates: hapten FP*a*, used in an earlier study for the generation of

324   polyclonal antibodies (Ceballos-Alcantarilla et al., 2015), and the new hapten FP*b* (Fig.

325   1a). In principle, the structures of the two haptens adequately mimic, both structurally

326   and electronically, the analyte, since they maintain integrally the structure and

327   functional groups thereof, incorporating a spacer arm for binding to the carrier protein

328   at opposed positions of the molecular skeleton, thus enabling antagonistic display

329   modes during the immune response. Additionally, two haptens (haptens FP*ha* and

330   FP*hb*), structurally heterologous from the previous ones (Fig. 1a), were also prepared

331   in order to evaluate their influence on the performance of the monoclonal antibody-

332   based cELISA. The former, in which the CF_2 group of the linker was replaced by a CH_2

333   group and the o*rtho*-CF_3 group in the distal aryl ring was shifted to the regioisomeric

334   *para*-position, had the same linker tethering site as hapten FP*a*, and the latter, in

335   which the CF_3 group of the proximal aryl ring was suppressed, held the linker at the

336   same site as hapten FP*b*.

337   The novel immunizing hapten FP*b* was prepared by a convergent synthetic

338   sequence, which involved the independent preparation of two appropriately

339   substituted aromatic moieties, the aryl moiety that incorporated the carboxylated C6

340   hydrocarbon chain that constituted the spacer arm and the substituted pyridine

341   system, which were joined together to complete the hapten skeleton in the final steps

342   of the synthesis (Fig. 2). The synthesis started with the commercially available

343   substituted benzoic acid **1**, which, after protection of the carboxylic group as a benzyl

344   ester, was transformed into aryl iodide **4**. This transformation involved reduction of

345   the nitro group to the corresponding amino group, using iron powder in acid medium,

346   followed by substitution of the amino group by iodine, using *tert*-butyl nitrite to

347   generate the corresponding 4-phenyl radical and diiodomethane as the source of

348   iodine. Subsequent palladium-catalysed Sonogashira cross-coupling reactions with the

349   terminal alkyne **5** took place under very smooth conditions affording the 4-alkenyl

350   derivative **6**. Completion of the introduction of the saturated hydrocarbon chain at the

351   C-4 position of the phenyl ring was undertaken by palladium catalysed heterogeneous

352   hydrogenation of the triple bond of compound **6** under low hydrogen pressure. Under

353   these conditions, we achieved not only complete hydrogenation of the triple bond but

354   also hydrogenolysis of the benzyl ester moiety to directly afford acid **7** in excellent

355   yield. The entire carbon framework of the target hapten FP*b* was completed by a

356   reaction of amidation between benzoic acid **7** and the amino group of previously

357   described amino pyridine **8** mediated by the phosphonium salt coupling reagent

358   PyAOP (Han & Kim, 2004). The synthesis of hapten FP*b* was completed by acid

359   catalysed hydrolysis of the *tert*-butyl ester moiety of amide **9**. Overall, the synthesis of

360   hapten FP*b* proceeded in 7 steps with an overall yield of *ca*. 27%.

361   The synthetic strategy used for the preparation of the heterologous assay

362　haptens, FP*ha* and FP*hb*, is based on the syntheses previously developed for the

363　preparation of the immunizing haptens, FP*a* and FP*b*, respectively. Their synthesis

364　involved the initial preparation of the aryl and heteroaromatic moieties, each with

365　appropriate functionalization at the different positions of the aromatic ring, which

366　were joined together to complete the skeleton of each hapten by an amidation

367　reaction (Fig. S2 and S3).

368　*3.2. Immunoreagent characterization*

369　　　　Haptens were activated through their transformation into the corresponding

370　*N*-hydroxysuccinimidyl esters using *N,N*-disuccinimidyl carbonate for subsequent

371　conjugation to carrier proteins. Since purified active esters of the haptens were

372　employed, the same coupling procedure was followed for the preparation of

373　immunizing and assay conjugates. Conjugate BSA–FP*b* was obtained with high yields

374　and an optimum MR of 16.5 was achieved, the same as the MR of conjugate BSA–FP*a*

375　which was previously reported (Ceballos-Alcantarilla et al., 2015). Regarding assay

376　conjugates, the MR values were 1.5, 4.5, and 4.5 for OVA–FP*b*, OVA–FP*ha*, and

377　OVA–FP*hb*, respectively, and 1.5 for the three prepared HRP conjugates. The

378　corresponding MALDI-TOF spectra are depicted in Fig. 3.

379　　　　A collection of monoclonal antibodies was generated; five from conjugate

380　BSA–FP*a*, namely FP*a*-type antibodies, and five from conjugate BSA–FP*b*, namely FP*b*-

381　type antibodies. All of them were characterized by checkerboard direct and indirect

382　cELISA using homologous and heterologous conjugates (conjugates carrying the same

383　or different hapten compared to the immunizing conjugate). Among FP*a*-type

384　antibodies, only FP*a*#12 afforded enough signal (higher than 0.8) in the direct assay

385   format (Table S1). The absence of signal was probably due to weak or no recognition of

386   the enzyme tracer by the antibody or to a loss of the antibody binding capacity upon

387   immobilization to the polystyrene surface of the microplate. Interestingly, antibody

388   FP*a*#12 bound the heterologous tracer of hapten FP*ha* but not the other heterologous

389   conjugates (FP*b* and FP*hb*). Regarding FP*b*-type antibodies in the direct assay format

390   (Table S1), the homologous tracer conjugate and, in most cases, tracer FP*hb* were

391   recognized. Haptens with opposite linker tethering sites were not bound by any of the

392   monoclonals in this format. The highest affinity was displayed by antibody FP*b*#12

393   together with tracer HRP–FP*b*, showing a subnanomolar value (IC_{50} = 0.75 nM).

394   As expected, all of the antibodies bound the homologous OVA coating

395   conjugate (Table S2). In this case, the obtained IC_{50} values for fluopyram were in the

396   low-to-mid nanomolar range. No differences were generally observed between FP*a*-

397   and FP*b*-type antibodies, indicating a similar capability of the two employed

398   immunogens to generate high-affinity binders. When binding to heterologous

399   conjugates occurred, it was exclusively to the heterologous conjugate with

400   homologous linker tethering site, i.e. the only heterologous conjugate recognized by

401   FP*a*-type antibodies was OVA–FP*ha* and the only heterologous conjugate recognized

402   by FP*b*-type antibodies was OVA–FP*hb*, with the exception of antibody FP*b*#32. As

403   observed for other small chemical molecules (Mercader, Parra, Esteve-Turrillas, Agulló,

404   Abad-Somovilla, & Abad-Fuentes, 2012; López-Moreno, Mercader, Agulló, Abad-

405   Somovilla, & Abad-Fuentes, 2014), linker location at an opposite site compared to the

406   homologous hapten constituted a harsh heterology, and the corresponding conjugate

407   was frequently not recognized by monoclonal antibodies. On the contrary, minor

408   modifications of the assay hapten framework generally help to increase the sensitivity

409   of the immunoassay, particularly if those changes affect a proximal site of the linker.

410   This trend agrees with that observed in this study; the modification of the

411   functionalization of the homoaromatic ring of hapten FP*hb* at a proximal site of the

412   linker did not hinder antibody binding, and the IC_{50} value could be reduced. However,

413   the combination of two changes at proximal and distal sites, such as those of hapten

414   FP*ha* – elimination of the geminal difluoride group and switch of the trifluoromethyl

415   position – probably caused that only a limited number of FP*a*-type antibodies

416   recognized this hapten. The highest sensitivity in this format (IC_{50} = 0.53 nM) was

417   observed with antibody FP*b*#12 combined with the heterologous OVA–FP*hb* conjugate.

418   In order to assess the specificity of the prepared monoclonal antibodies,

419   indirect cELISA tests were carried out using the homologous conjugate. A series of

420   different analytes were evaluated including fungicides of the SDHI family

421   (penthiopyrad, boscalid, and fluxapyroxad), the main metabolite of fluopyram (2-

422   (trifluoromethyl)benzamide, also called M25), tebuconazole, which is coformulated in

423   Luna® Experience together with fluopyram, and other pesticides commonly found in

424   fruit samples, such as fluopicolide, fenhexamid, cyprodinil, fludioxonil, azoxystrobin,

425   and trifloxystrobin. FP*b*-type antibodies showed high specificity and no remarkable

426   inhibition was observed with any of the studied molecules; just cross-reactivities below

427   1% were seen for a few antibodies with SDHI compounds and fluopicolide (Table S3).

428   Interestingly, all of the FP*a*-type antibodies showed moderate or slight cross-reactivity

429   with   fluopicolide.   Fluopyram   and   fluopicolide   share   the   3-chloro-5-

430   (trifluoromethyl)pyridin-2-yl moiety which probably explains the observed cross-

431   reactivity. However, it was surprising that those antibodies that were obtained using a

432   hapten with the linker located at such heteroaromatic ring (FP*a*-type) recognized

19

433   fluopicolide, whereas it was not or only slightly bound by FP*b*-type antibodies

434   generated from a hapten displaying such immunodeterminant moiety at a distal

435   position of the spacer arm. Apparently, this result seems to contradict the

436   Landsteiner's principle (Landsteiner, 1962). However, it is possible that haptens can

437   adopt a folded conformation, similar to the more stable conformation of fluopyram

438   itself (Fig. 1b), so that during the immune response the common immunogenic

439   elements with fluopicolide are more exposed in hapten FP*a* than in hapten FP*b*,

440   resulting in the generation of antibodies with higher cross-reactivity to fluopicolide

441   from the former than from the latter.

442   *3.3. Immunoassay characterization*

443   Two immunoassays were selected for further development and validation using

444   monoclonal antibody FP*b*#12 in combination with the homologous tracer conjugate for

445   the direct cELISA format and the heterologous OVA–FP*hb* conjugate for the indirect

446   format. The IC_{50} values of these assays were one order of magnitude lower than the

447   best values previously published with polyclonal antibodies (Ceballos-Alcantarilla et al.,

448   2015). Immunoreagent concentrations were optimized in order to reach A_{max} values

449   around 1.0. Moreover, the influence of pH and ionic strength of the immunoreaction

450   buffer was studied. With the direct assay, the A_{max} and the IC_{50} values smoothly

451   decreased at pH values lower and higher than PBS (Fig. S4). On the other hand, minute

452   influence was found over the A_{max} value of the indirect assay only at basic pHs. The IC_{50}

453   value of this assay was little altered at acidic pH values but it rapidly decreased at basic

454   pHs. Regarding the ionic strength, minimal effects were observed over the direct

455   assay; the A_{max} and IC_{50} values were only slightly lowered at I = 50 mM. With the

456 indirect assay, low influence was observed over the A_{max} value in the studied salt

457 concentration range; however, low ionic strength values sharply raised the IC_{50} value

458 whereas it was decreased at salt concentrations higher than PBS.

459 Tolerance of the selected immunoassays to the presence of methanol, ethanol,

460 and acetonitrile was evaluated. In the studied concentration range, both

461 immunoassays were quite tolerant to these solvents, even to acetonitrile which usually

462 strongly influences negatively the analytical parameters of immunoassays (Fig. S5).

463 Lower variation of the A_{max} and IC_{50} values were observed with the indirect assay than

464 with the direct assay. For the former, higher solvent contents slightly increased the

465 A_{max} value, whereas little changes of the IC_{50} value were observed along the studied

466 solvent concentration range. For the latter assay, increasing solvent concentrations

467 moderately raised the A_{max} value and the IC_{50} value was doubled or more at 5% (v/v)

468 solvent contents.

469 The optimized assay parameters of the selected immunoassays are listed in Table

470 1. Both immunoassays showed high sensitivity to fluopyram, with IC_{50} values around

471 0.2 µg L^{-1} and LOD values in the nanogram per litre scale. The theoretical working

472 range of the standard curve was calculated as the IC_{20}–IC_{80} interval, and covered about

473 one order of magnitude. Moreover, the direct assay showed excellent precision of the

474 A_{max} value for inter-day and intra-day determinations but a slight deviation of the IC_{50}

475 values was observed in both cases. For the indirect assay, the values of the two assay

476 parameters (A_{max} and IC_{50}) were highly precise for inter-day and intra-day

477 measurements.

478 *3.4. Recovery studies*

479   These studies were carried out with fluopyram-free samples of a stone fruit

480   (plums), three varieties of red grapes (Bobal, Garnacha, and Tempranillo), and one

481   variety of white grapes (Macabeo), all of them directly collected from the fields.

482   Moreover, blank musts and wines of the four grape varieties were prepared. For

483   winemaking, glucose and fructose concentration as well as glycerol, ethanol, and

484   acetic acid contents were measured (Table S4). Fermentation was monitored by

485   measuring the must density, and the process was considered completed at 0.998 g

486   mL^{-1} (time of fermentation was between 140 and 170 h). The Bobal must variety had

487   the lowest carbohydrate contents, whereas the Macabeo must contained double

488   amount of glycerol than the Bobal must. The obtained wines showed reduced contents

489   of glucose and fructose, as expected, and contained between 10.0% and 12.5% ethanol

490   (v/v), as many commercial wines. The glycerol and acetic acid concentrations were

491   similar in the four wines.

492   A preliminary study was carried out to estimate the matrix effects of plum and

493   grape extracts, must, and wine of the four varieties over the optimized immunoassays.

494   As depicted in Fig. S6, variations of the A_{max} value higher than 20% were only observed

495   at low dilution factors for all fruit extracts in the direct assay, and low matrix effects

496   were generally found with fruit samples in the indirect assay. On the contrary, lower

497   matrix effects were observed with must samples in the direct assay than in the indirect

498   format, particularly with Garnacha and Tempranillo musts. Finally, the A_{max} value

499   slightly increased with the lowest dilutions of wine samples in the direct assay but

500   higher matrix effects occurred in the indirect format, particularly with Garnacha and

501   Bobal wine samples.

502   Blank samples of the described foodstuffs were fortified with fluopyram from 5 to

503   500 µg L^{-1}, diluted 1/25, 1/50, and 1/150, and analysed by the two described

504   immunoassays. Raw data are listed in Table S5 and S6, and average values are

505   summarized in Table 2. Excellent recoveries and CV values below 20% were found with

506   all of the studied samples when the direct assay was employed. With the indirect

507   assay, excellent recoveries were obtained with CV values below 20% for plum and all

508   grape extracts, the Macabeo white must, and the four wine varieties (Table S6). For

509   red musts with the indirect assay, recoveries were generally between 70% and 90% for

510   Bobal and Garnacha varieties, or below 70% for Tempranillo must, and CV values were

511   below 20%.

512   The experimental LOQs for plum and grape extracts of the four varieties were 5

513   µg L^{-1} with both immunoassays (Tables S5 and S6), which is much lower than the

514   maximum residue limits set by the EU (0.5 mg kg^{-1} for plums and at 1.5 mg kg^{-1} for

515   wine grapes) and the US (0.5 mg kg^{-1} for plums and 2.0 mg kg^{-1} for wine grapes) (EU

516   Pesticide Database, 2019; Global MRL Database, 2019). For must and wine samples,

517   the LOQs with the direct assay were either 5 or 10 µg L^{-1}, depending on the variety,

518   except for the Garnacha wine, with the darkest red colour, which was 50 µg L^{-1}.

519   Concerning the indirect assay, the LOQ for the Macabeo white must was 5 µg L^{-1}.

520   Matrix effects from red must varieties seemed to occur in this immunoassay, so no

521   LOQ could be established according to the previously described definition. The LOQs

522   for wine samples in this format were either 5 or 10 µg L^{-1}, depending on the variety.

523   *3.5. Validation studies*

524   Fluopyram concentration in in-field treated samples was determined both by

525   UPLC–MS/MS, as a reference chromatographic method, and by the developed

526   immunoassays. The obtained values (Table S7) were statistically compared by Deming

527   regression and Bland-Altman dispersion analysis. The regression line for the direct

528   immunoassay was y = 1.014x−0.142, with a 95% confidence interval from 0.978 to

529   1.050 for the slope and from −0.633 to 0.349 for the intercept, so those values were

530   statistically equal to 1 and 0, respectively (Fig. 4a). Therefore, a good correlation

531   between the chromatographic and immunochemical results of the direct assay exists.

532   The regression line for the indirect assay was y = 0.902x+0.227, with a 95% confidence

533   interval from 0.873 to 0.930 for the slope and from −0.275 to 0.730 for the intercept.

534   In this case, the slope was slightly lower than 1 and the intercept was statistically equal

535   to 0. This result suggests certain underestimation of the fluopyram concentration by

536   the indirect immunoassay. According to the Bland-Altman plots (Fig. 4b), only random

537   deviations exist between chromatographic and immunochemical results of both

538   immunoassays; the experimental values were mainly within the limits of agreement

539   (mean ± 1.96s) and they were arbitrarily distributed above and below the average line.

540   A t-Student analysis indicated that the mean difference between both methods was

541   not statistically different from 0 for the direct assay whereas a bias of −7 µg L^{-1} was

542   revealed for the indirect immunoassay.

543   **4. Conclusions**

544   Novel haptens of fluopyram have been prepared and specific high-affinity

545   monoclonal antibodies to this new-generation SDHI fungicide have been raised for the

546   first time. Different types of heterologous haptens were studied. Most monoclonals

547   bound heterologous conjugates in which the heterologies were introduced at a

548   proximal site of the linker, whereas heterologous haptens with the linker at an

549   opposite position seemed to hinder monoclonal antibody binding. Preparation of

550   haptens with a homologous linker site and a heterology at a proximal position was

551   shown to be a good approach for enhancing immunoassay sensitivity in both the direct

552   and the indirect assay formats. Two immunoassays using different cELISA formats were

553   characterized and optimized, showing good performance for the analysis of fluopyram

554   in fortified plum and grape samples of four varieties as well as the corresponding in-

555   house prepared musts and wines. Statistical analysis of results demonstrated good

556   agreement between a reference chromatographic method and the developed

557   immunoassays, particularly the direct assay.

570   **Appendix A. Abbreviations used**

571   BSA: bovine serum albumin; cELISA: competitive enzyme-linked immunosorbent

572 assay; CV: coefficient of variation; HRP: horseradish peroxidase; LOD: limit of

573 detection; LOQ: limit of quantification; MALDI-TOF: matrix-assisted laser desorption

574 ionization time-of-flight mass spectrometry; MR: molar ratio; OVA: ovalbumin; PB:

575 phosphate buffer; PBS: phosphate buffered saline; PBST: PBS containing Tween 20;

576 SDHI: succinate dehydrogenase inhibitor; TPP: triphenyl phosphate; UPLC–MS/MS:

577 ultra-high performance liquid chromatography coupled to tandem mass spectrometry.

578 **Appendix B. Supplementary material**

579   Supplementary data associated with this article can be found, in the online version,

580 at

581 **References**

582 Abad-Fuentes, A., Ceballos-Alcantarilla, E., Mercader, J. V., Agulló, C., Abad-Somovilla,

583   A., & Esteve-Turrillas, F. A. (2015). Determination of succinate-dehydrogenase-

584   inhibitor fungicide residues in fruits and vegetables by liquid chromatography–

585   tandem mass spectrometry. *Analytical & Bioanalytical Chemistry*, *407*(14), 4207–

586   4211.

587 Avenot, H. F. & Michailides, T. J. (2010). Progress in understanding molecular

588   mechanisms and evolution of resistance to succinate dehydrogenase inhibiting

589   (SDHI) fungicides in phytopathogenic fungi. *Crop Protection*, *29*, 643–651.

590 Ceballos-Alcantarilla, E., Agulló, C., Abad-Fuentes, A., Abad-Somovilla, A., & Mercader,

591   J. V. (2015). Rational design of a fluopyram hapten and preparation of bioconjugates

592   and antibodies for immunoanalysis. *RSC Advances*, *5,* 51337–51341.

593   Dzuman, Z., Zachariasova, M., Veprikova, Z., Godula, M., & Hajslova, J. (2015). Multi-

594   analyte high performance liquid chromatography coupled to high resolution

595   tandem mass spectrometry method for control of pesticide residues, mycotoxins,

596   and pyrrolizidine alkaloids. *Analytica Chimica Acta*, *863*, 29–40.

597   Esteve-Turrillas, F. A., Parra, J., Abad-Fuentes, A., Agulló, C., Abad-Somovilla, A., &

598   Mercader, J. V. (2010). Hapten synthesis, monoclonal antibody generation, and

599   development of competitive immunoassays for the analysis of picoxystrobin in beer.

600   *Analytica Chimica Acta*, *682*, 93–103.

601   EU Pesticide Database. (2019). http://ec.europa.eu/food/plant/pesticides/eu-

602   pesticides-database/public/?event=_homepage&language=EN Accessed 8 January

603   2019.

604   European Commission Regulation. (2013). Commission implementing regulation (EU)

605   No 802/2013 of 22 August 2013 approving the active substance fluopyram, in

606   accordance with Regulation (EC) No 1107/2009 of the European Parliament and of

607   the Council concerning the placing of plant protection products on the market, and

608   amending the Annex to Commission Implementing Regulation (EU) No 540/2011.

609   *Official Journal of the European Union*, *L225*, 13–16.

610   European Food Safety Authority. (2011). Setting of new MRLs and import tolerances

611   for fluopyram in various crops. *EFSA Journal*, *9*(9), 2388.

612   European Food Safety Authority. (2013). Conclusion on the peer review of the

613   pesticide risk assessment of the active substance fluopyram. *EFSA Journal*, *11*(4),

614   3052.

615   European Food Safety Authority. (2015). Scientific Report of EFSA. The 2013 European

616   Union report on pesticide residues in food. *EFSA Journal*, *13*(3), 4038.

617   Gan, J., Lv, L., Peng, J., Li, J., Xiong, Z., Chen, D., & He, L. (2016). Multi-residue method

618   for the determination of organofluorine pesticides in fish tissue by liquid

619   chromatography triple quadrupole tandem mass spectrometry. *Food Chemistry*,

620   *207*, 195–204.

621   Global MRL Database. (2019). https://www.globalmrl.com/home/ Accessed 8 January

622   2019.

623   Han, S.-Y. & Kim, Y.-A. (2004). Recent development of peptide coupling reagents in

624   organic synthesis. *Tetrahedron*, *60*, 2447–2467.

625   Landsteiner, K. (1962). *The specifity of serological reactions* (Rev. Ed.). New York: Dover

626   Publications.

627   Lee, J., Kim, L., Shin, Y., Lee, J., Lee, J., Kim, E., Moon, J. K., & Kim, J. H. (2017). Rapid

628   and simultaneous analysis of 360 pesticides in brown rice, spinach, orange, and

629   potato using microbore GC–MS/MS. *Journal of Agricultural and Food Chemistry*,

630   *65*(16), 3387–3395.

631   López-Moreno, R., Mercader, J. V., Agulló, C., Abad-Somovilla, A., & Abad-Fuentes, A.

632   (2014). Immunoassays for trifloxystrobin analysis. Part I. Rational design of

633   regioisomeric haptens and production of monoclonal antibodies. *Food Chemistry*,

634   *152*, 230–236.

635   Lozano, A., Kiedrowska, B., Scholten, J., de Kroon, M., de Kok, A., & Fernández-Alba, A.

636   R. (2016). Miniaturisation and optimisation of the Dutch mini-Luke extraction

637   method for implementation in the routine multi-residue analysis of pesticides in

638   fruits and vegetables. *Food Chemistry*, *192*, 668–681.

639 Mercader, J. V., Parra, J., Esteve-Turrillas, F. A., Agulló, C., Abad-Somovilla, A., & Abad-

640 Fuentes, A. (2012). Development of monoclonal antibody-based competitive

641 immunoassays for the detection of picoxystrobin in cereal and oilseed flours. *Food*

642 *Control*, *26*, 162–168.

643 Mercader, J. V., Suárez-Pantaleón, C., Agulló, C., Abad-Somovilla, A., & Abad-Fuentes,

644 A. (2008a). Hapten synthesis and monoclonal antibody-based immunoassay

645 development for detection of the fungicide trifloxystrobin. *Journal of Agricultural*

646 *and Food Chemistry*, *56*, 2581–2588.

647 Mercader, J. V., Suárez-Pantaleón, C., Agulló, C., Abad-Somovilla, A., & Abad-Fuentes,

648 A. (2008b). Production and characterization of monoclonal antibodies specific to the

649 strobilurin pesticide pyraclostrobin. *Journal of Agricultural and Food Chemistry*, *56*,

650 7682–7690.

651 Pesticide Properties Database. (2019).

652 https://sitem.herts.ac.uk/aeru/ppdb/en/index.htm Accessed 8 January 2019.

653 Pfeil, R. & Boobis, A. (2010). Fluopyram. In *Joint Meeting of the FAO Panel of Experts*

654 *on Pesticide Residues in Food and the Environment and the WHO Core Assessment*

655 *Group on Pesticide Residues*. *Pesticide residues in food 2010. Toxicological*

656 *evaluations* (pp. 383–468). Rome: WHO Press.

657 Polgár, L., García-Reyes, J. F., Fodor, P., Gyepes, A., Dernovics, M., Abrankó, L., Gilbert-

658 López, B., & Molina-Díaz, A. (2012). Retrospective screening of relevant pesticide

659 metabolites in food using liquid chromatography high resolution mass spectrometry

660 and accurate-mass databases of parent molecules and diagnostic fragment ions.

661 *Journal of Chromatography A*, *1249*, 83–91.

662   Proffer, T. J., Lizotte, E., Rothwell, N. L., & Sundin, G. W. (2013). Evaluation of dodine,

663   fluopyram and penthiopyrad for the management of leaf spot and powdery mildew

664   of tart cherry, and fungicide sensitivity screening of Michigan populations of

665   *Blumeriella jaapii. Pest Management Science*, *69*(6), 747–754.

666   Yang, P., Chang, J. S., Wong, J., Zhang, K., Krynitsky, A. J., Bromirski, M., & Wang, J.

667   (2015). Effect of sample dilution on matrix effects in pesticide analysis of several

668   matrices by liquid chromatography–high-resolution mass spectrometry. *Journal of*

669   *Agricultural and Food Chemistry*, *63*(21), 5169–5177.

670   **Figure captions**

671   **Fig. 1**. a) Molecular structures of fluopyram, immunizing haptens (FP*a* and FP*b*), and

672   heterologous assay haptens (FP*ha* and FP*hb*). b) Global minimum energy conformation

673   of fluopyram. Calculations were performed using Molecular Mechanics (MM3) as

674   implemented in the CAChe program. A systematic conformational search was

675   performed (all rotatable bonds were rotated by 24° degree steps) and the geometry of

676   the generated more stable conformer was refined by performing an optimized

677   geometry calculation in MOPAC using PM3 parameters. The elements are represented

678   in the following manner: carbon, grey; oxygen, red; nitrogen, blue; chlorine, yellow;

679   fluorine, green. The dashed line denotes an intramolecular hydrogen bond between

680   the pyridine nitrogen atom and the hydrogen atom of the amide moiety. This bond

681   could be reinforced by simultaneous interaction of the same hydrogen with the

682   fluorine atoms of the spatially proximal CF_3 group.

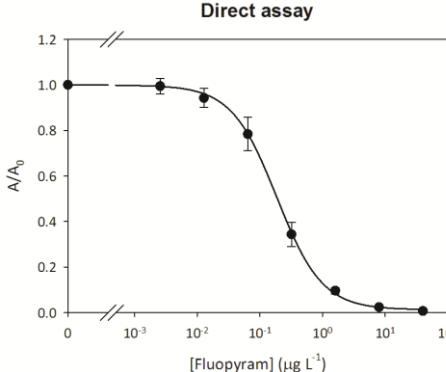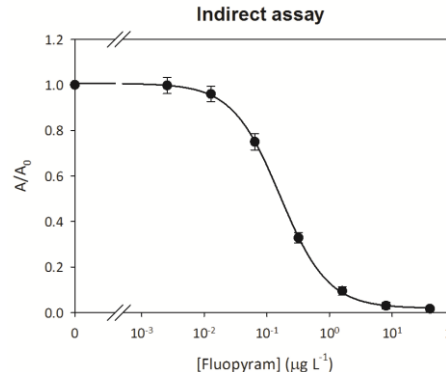683   **Fig. 2**. Synthetic sequence for the preparation of hapten FP*b*.

684   **Fig. 3.** MALDI-TOF spectra of proteins (blue) and the corresponding conjugates with

685   haptens FP*b* (green), FP*ha* (orange), and FP*hb* (cyan). a) BSA conjugate; b) OVA

686   conjugates; c) HRP conjugates.

687   **Fig. 4.** a) Deming regression plots for comparison of results from the analysis of in-field

688   treated plums (solid symbols) and grapes (open symbols) obtained by a reference

689   chromatographic technique and the developed direct and indirect cELISA. The solid

690   line represents the regression line and the dashed lines are the 95% confidence

691   interval. b) Bland-Altman dispersion plots depicting the average difference between

692   determinations of the compared methods (solid line) and the ±1.96s limits (dashed

693   lines). The mean difference was 3.6 µg L^{-1} for the direct assay and −7.7 µg L^{-1} for the

694   indirect assay. ELISA values are the mean of 5 independent determinations while HPLC

695   values are the mean of two replicates.

Highlights

- Fluopyram regioisomeric haptens with opposite linker tethering sites were used.

- High-affinity monoclonal antibodies to fluopyram were generated for the first time.

- Two ELISAs were optimized for fluopyram analysis with LOD values below 0.05 µg L^{-1}.

- Immunoassay performance was verified in plum, grape, must, and wine samples.

- Immunochemical results were validated with LC-MS using contaminated samples.

Table(s)

Table 1. Normalized standard curves, assay conditions, and analytical parameters of the developed immunoassays for fluopyram analysis (n = 12).

	Direct assay	Indirect assay
Antibody	FPb#12 at 1000 µg L^{-1}	FPb#12 at 30 µg L^{-1}
Conjugate	HRP–FPb at 30 µg L^{-1}	OVA–FPhb at 1000 µg L^{-1}
Buffer	pH 7.4, I = 166 mM	pH 7.4, I = 166 mM
A_{max}	1.187 ± 0.124	1.001 ± 0.055
IC_{50} (µg L^{-1})	0.187 ± 0.046	0.162 ± 0.016
Slope	−1.201 ± 0.163	−1.139 ± 0.083
A_{min}	0.015 ± 0.012	0.019 ± 0.015
LOD (µg L^{-1})	0.031 ± 0.014	0.024 ± 0.004
LR (µg L^{-1})[a]	from 0.060 ± 0.022 to 0.595 ± 0.112	from 0.048 ± 0.007 to 0.554 ± 0.066
CV inter-day (%)[b]		
A_{max}	8	5
IC_{50}	25	8
CV intra-day (%)[b]		
A_{max}	9	3
IC_{50}	11	8

[a] Linear range calculated as the IC_{20}–IC_{80} interval. [b] Inter-day and intra-day precision calculated as de coefficient of variation of 4 independent repeats.

Table 2. Average recovery values and coefficients of variation obtained by the two optimized cELISAs for fluopyram fortified plum and grape extracts, must, and wine samples of different varieties (n = 5).
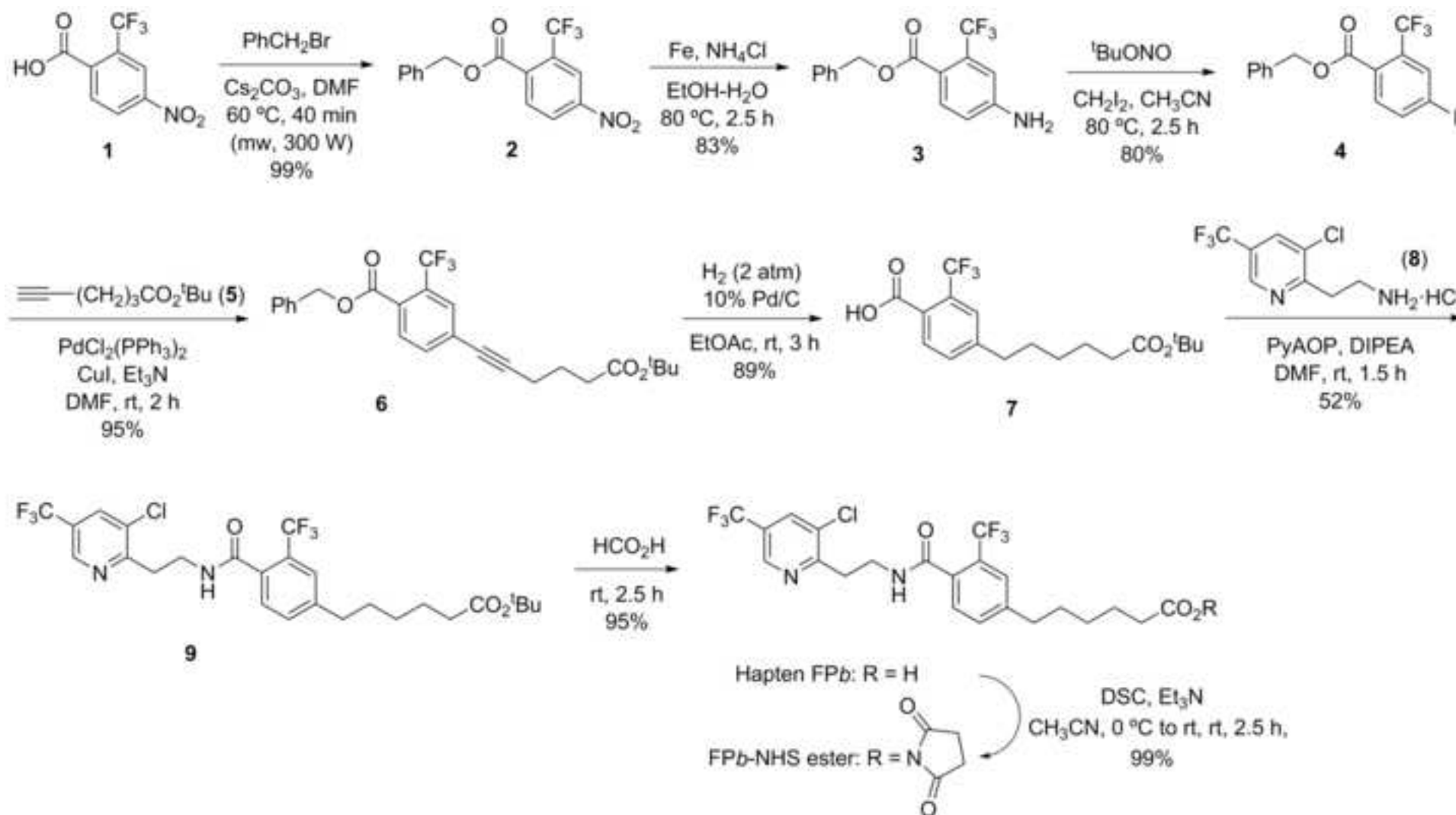
Matrix	Variety	Immunoassays for fluopyram			
		Direct		Indirect	
		R (%, ±s)[a]	CV (%, ±s)[b]	R (%, ±s)	CV (%, ±s)
Plum	-	103.4 ± 7.6	9.8 ± 3.8	94.8 ± 8.6	8.0 ± 2.7
Grape	Bobal	102.8 ± 7.9	6.0 ± 2.6	100.2 ± 4.2	6.6 ± 4.2
	Garnacha	102.0 ± 2.8	5.7 ± 2.8	97.5 ± 6.9	8.5 ± 6.5
	Tempranillo	103.7 ± 10.8	9.4 ± 4.3	102.3 ± 11.5	8.9 ± 6.1
	Macabeo	100.8 ± 4.6	12.1 ± 4.6	96.0 ± 10.0	7.5 ± 3.6
Must	Bobal	104.4 ± 6.2	6.8 ± 2.9	76.3 ± 8.1	12.5 ± 2.3
	Garnacha	108.5 ± 9.3	11.1 ± 4.8	78.5 ± 6.7	12.1 ± 2.6
	Tempranillo	109.6 ± 5.8	13.4 ± 4.0	-[c]	-
	Macabeo	108.6 ± 11.4	9.6 ± 4.7	98.7 ± 3.9	8.7 ± 5.5
Wine	Bobal	101.2 ± 9.2	12.3 ± 4.9	95.0 ± 8.9	17.1 ± 2.8
	Garnacha	108.5 ± 4.4	15.7 ± 2.9	87.0 ± 3.2	13.3 ± 3.7
	Tempranillo	106.4 ± 5.1	12.9 ± 3.4	93.6 ± 6.3	11.4 ± 2.4
	Macabeo	108.2 ± 9.3	6.2 ± 3.3	100.3 ± 3.7	12.2 ± 4.4

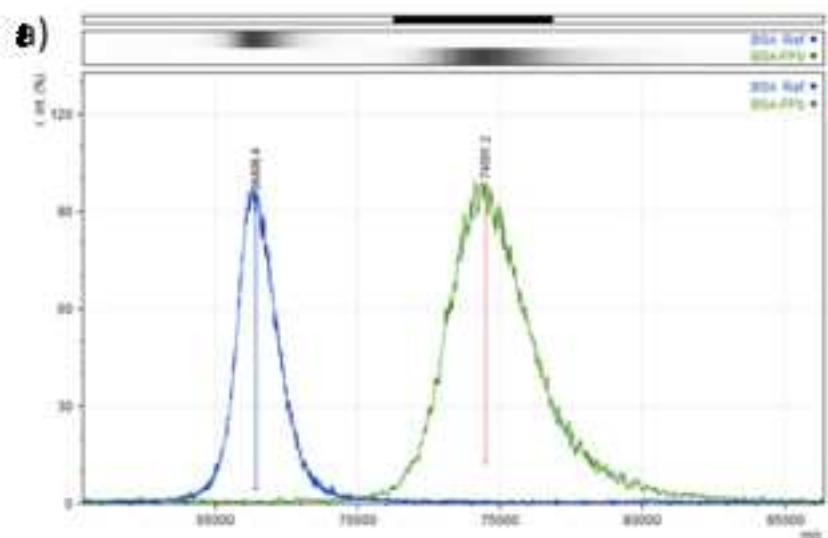[a] Average recovery values. [b] Average coefficients of variation. [c] Out of range.
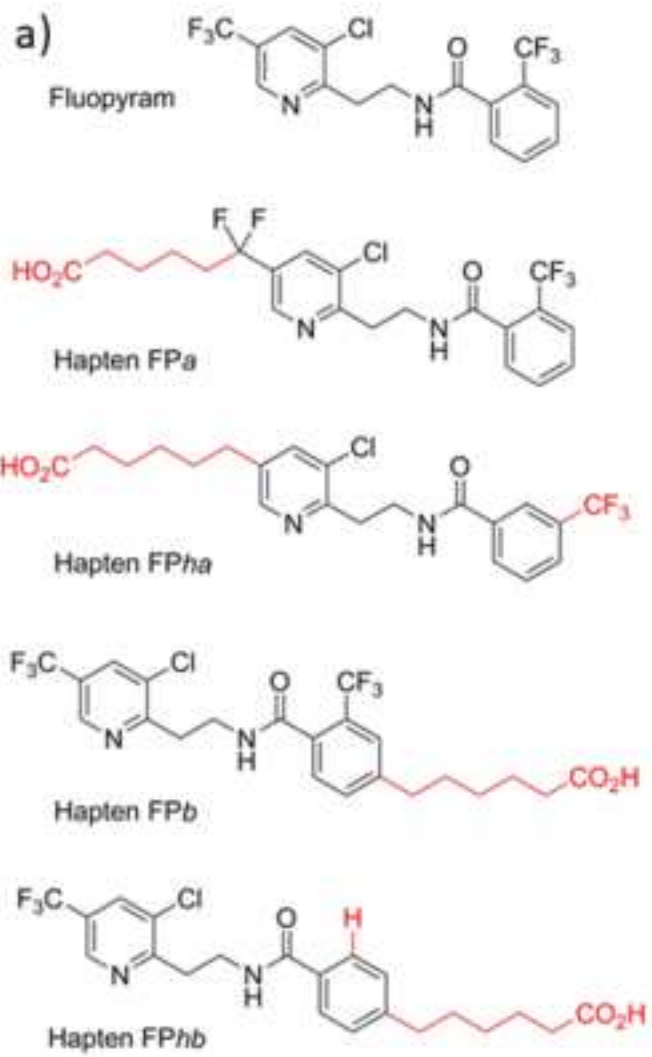
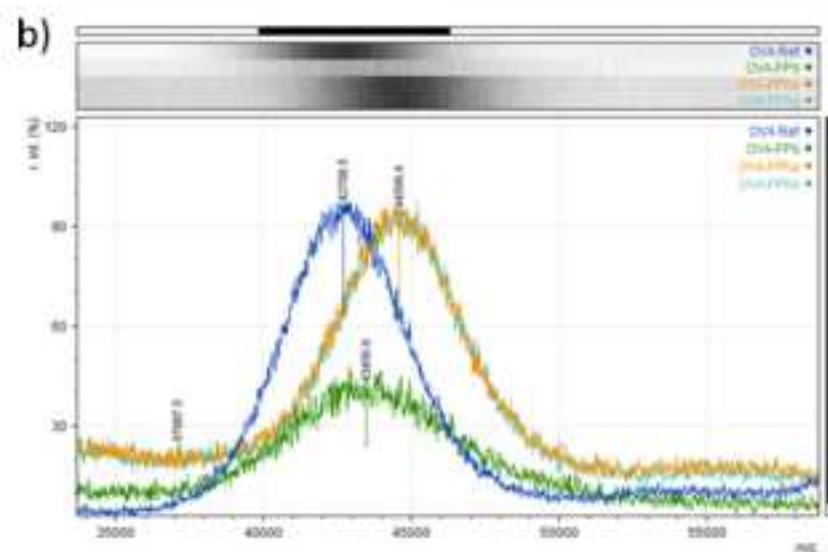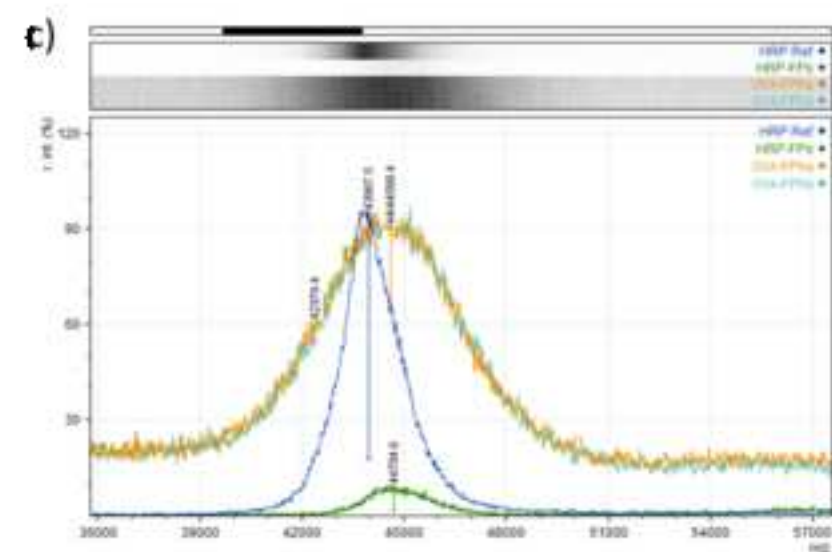**Figure(s)**
Click here to download high resolution image

a)

Fluopyram

Hapten FPa

Hapten FPha

Hapten FPb

Hapten FPhb

b)

a)

	m/z	Δm/hapten	Δ(m/z)	MR
BSA	66406	-	-	-
BSA-FPb	74502	492.1	8095	16.5

b)

	m/z	Δm/hapten	Δ(m/z)	MR
OVA	42708	-	-	-
OVA-FPb	43457	492.1	748	1.5
OVA-FPha	44596	424.1	1888	4.5
OVA-FPhb	44598	424.1	1889	4.5

c)

	m/z	Δm/hapten	Δ(m/z)	MR
HRP	43967	-	-	-
HRP-FPb	44705	492.1	737	1.5
HRP-FPha	44590	424.1	623	1.5
HRP-FPhb	44604	424.1	636	1.5
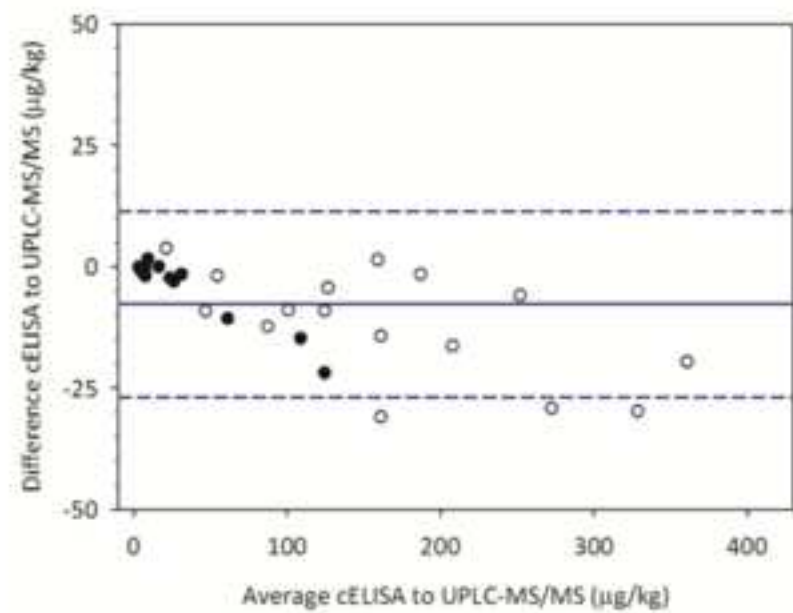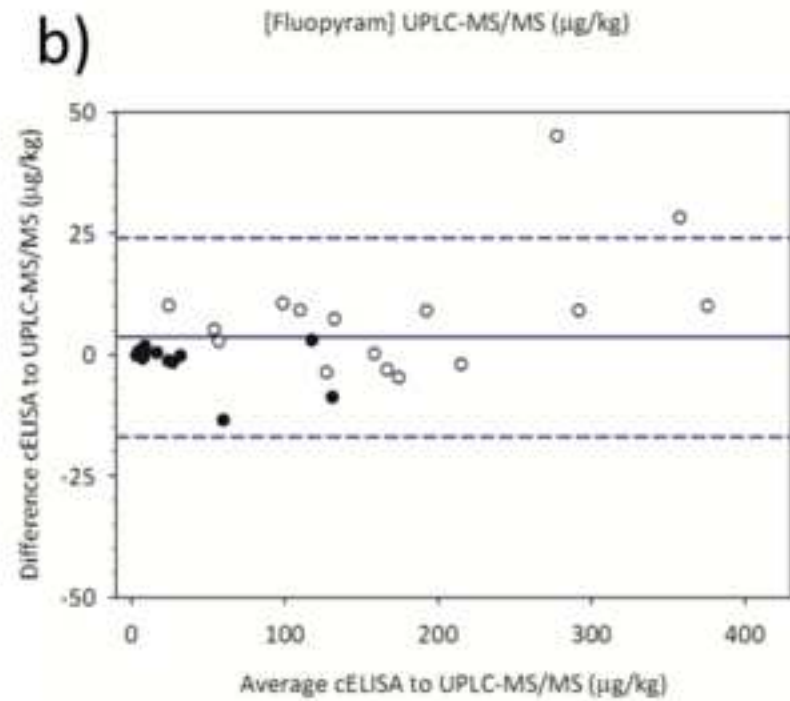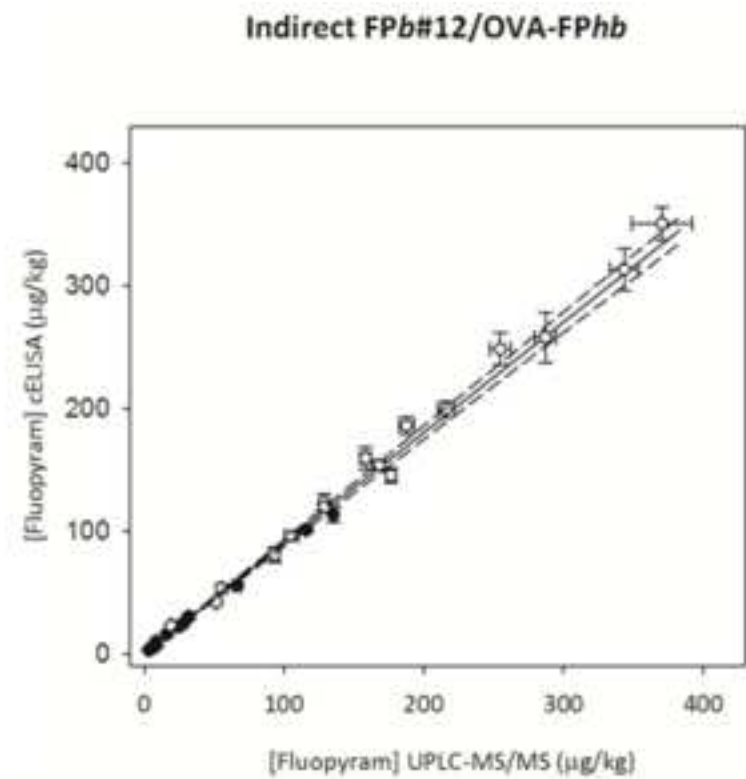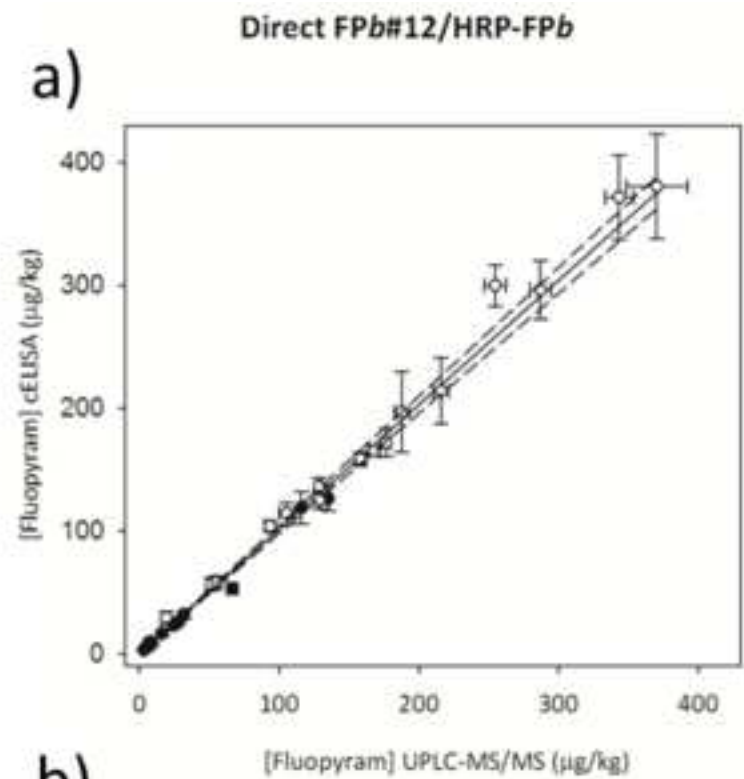
Supplementary Material

Declaration of interests

☒ The authors declare that they have no known competing financial interests or personal relationships that could have appeared to influence the work reported in this paper.

☐The authors declare the following financial interests/personal relationships which may be considered as potential competing interests: